RESEARCH ARTICLE

ASPN Synergizes with HAPLN1 to Inhibit the Osteogenic Differentiation of Bone Marrow Mesenchymal Stromal Cells and Extracellular Matrix Mineralization of Osteoblasts

Guohui Zhou, B.D[1], Xinmin Yan, M.D[1], Zhenfei Chen, B.D[2], Xing Zeng, B.D[1], Fangqian Wu, B.A.[3]

Department of [1]Orthopaedics, [2]Hospital-Acquired Infection Control Department and [3]Spine Surgery, First People's Hospital of Fuzhou, Fuzhou, China

Objective: Bone marrow mesenchymal stromal cells (BMSCs) are major sources of osteogenic precursor cells in bone remodeling, which directly participate in osteoporosis (OP) progression. However, the involved specific mechanisms of BMSCs in OP warrant mass investigations. Initially, our bioinformatics analysis uncovered the prominent up-regulation of Asporin (ASPN) and proteoglycan link protein 1 (HAPLN1) in osteoblasts (OBs) of OP patients and their possible protein interaction. Hence, this study aimed to explore the effects of ASPN and HAPLN1 on osteogenic differentiation of BMSCs, extracellular matrix (ECM) mineralization of OBs, and osteoclastogenesis, hoping to offer research basis for OP treatment.

Methods: GSE156508 dataset was used for analysis and screening to acquire the differentially expressed genes in OBs of OP patients, followed by the predicative analysis *via* STRING. OP mouse models were induced by ovariectomy (OVX), and ASPN and HAPLN1 expression was determined. BMSCs and bone marrow macrophages (BMMs) were isolated from OVX mice and induced for osteogenic differentiation and osteoclastogenesis, respectively. After knockdown experiments, we assessed adipogenic differentiation and osteogenic differentiation in BMSCs. Osteogenic (OPN, OCN, and COL1A1) and osteoclast (Nfatc1 and c-Fos) marker protein expression was determined. The binding of ASPN to HAPLN1 was analyzed.

Results: High expression of ASPN and HAPLN1 and their protein interaction were observed in OBs of OP patients *via* bioinformatics and in bone tissues of OVX mice. ASPN interacted with HAPLN1 in BMSCs of OVX mice. ASPN/HAPLN1 knockdown increased ALP, OPN, OCN, and COL1A1 protein expression and ECM mineralization in BMSCs while decreasing Nfatc1 and c-Fos expression in BMMs. These effects were aggravated by the simultaneous knockdown of ASPN and HAPLN1.

Conclusion: Our results indicate that ASPN synergises with HAPLN1 to suppress the osteogenic differentiation of BMSCs and ECM mineralization of OBs and promote the osteoclastogenesis in OP.

Key words: ASPN; Bone marrow mesenchymal stromal cells; HAPLN1; Osteogenic differentiation; Osteoporosis

Introduction

Osteoporosis (OP) is a chronic musculoskeletal disease characterized by bone mass reduction and microstructure destruction,[1] giving rise to devastating sequelae, disability, and even mortality.[2] Currently used treatment methods for OP, including hormone replacement therapy and use of selective estrogen receptor modulators and mineral agents (strontium ranelate), can contribute to adverse

Address for correspondence Fangqian Wu, B.A, Department of Spine Surgery, First People's Hospital of Fuzhou, No. 1099 Yingbin Avenue, Fuzhou, Jiangxi, P.R. China 344000; Email: wuqianfang123@163.com

Received 14 October 2022; accepted 24 May 2023

side effects.[3] Hence, novel therapeutic strategies are urgently required for OP treatment. Bone marrow mesenchymal stem cells (BMSCs) can differentiate into multiple types of cells, including osteoblasts (OBs), and their differentiation into OBs is called osteogenic differentiation, which is involved in the formation of bones.[1] Osteogenic differentiation of BMSCs is inhibited during OP progression, and recovery of this process decreases the bone loss in OP.[2,3] Extracellular matrix (ECM) mineralization significantly affects the bone strength (resistance to bone fracture), and it is decreased in patients with OP.[4] These reports suggest the potential value of molecules related to the osteogenic differentiation of BMSCs and ECM mineralization as targets in OP treatment.

Asporin (ASPN), also known as the periodontal ligament-associated protein-1 (PLAP-1), is a key member of the class I small leucine-rich proteoglycan family that is associated with the pathogenesis of bone degenerative diseases.[5] ASPN deficiency ameliorates high-fat diet-induced alveolar bone loss.[6] Moreover, ectopic expression of ASPN suppresses the differentiation of BMSCs into OB-like cells.[7] Li *et al.* reported the upregulation of ASPN expression in glucocorticoid-induced OP.[8] Interestingly, ASPN and hyaluronan and proteoglycan link protein 1 (HAPLN1) have been reported to be associated with the pathogenesis of intervertebral disc degeneration.[9] In our study, Search Tool for the Retrieval of Interacting Genes/Proteins (STRING) revealed the protein interaction between ASPN and HAPLN1. HAPLN1 is a hyaluronan-binding protein that plays an essential role in cartilage proteoglycan preparation.[10] HAPLN1 is also involved in spinal osteophyte formation[11] and is a pivotal ECM-related molecule.[12] Furthermore, HAPLN1 is overexpressed in some musculoskeletal diseases, such as rheumatoid arthritis.[13] Based on these findings, we performed various experiments using isolated BMSCs from OP mice in this study to validate the following contents: (i) the role and expression of ASPN and HAPLN1 in osteogenic differentiation of BMSCs, ECM mineralization of OBs, and osteoclast differentiation of bone marrow macrophages (BMMs) in OP; (ii) the binding relationship between ASPN and HAPLN1.

Materials and Methods

Bioinformatics Analysis

In this study, we downloaded dataset GSE156508, including data of six healthy controls and six patients with OP, from the Gene Expression Omnibus (GEO) database. Primary OBs were extracted from partial hip bones of patients in these two groups for gene expression analysis. RStudio was used to analyze the GSE156508 dataset, and $|\log FC| > 1$ and $P < 0.05$ were used to screen the differentially expressed genes. Protein interactions among all highly expressed genes were predicted using STRING database (http:/string-db.org) and a protein interaction between ASPN and HAPLN1 was observed in patients with OP. We also identified the ECM-related genes using PathCard (https://pathcards.genecards.org/)[14] as follows: PathCard website was opened and "ECM" was input in the search box to identify pathways meeting the search criteria. Next, genes included in this pathway were obtained and pasted on the STRING website (https://cn.string-db.org/cgi/input?sessionId=bTumjNJV7YRV&input_page_show_search=off) for analysis. Finally, Cytoscape was used for plotting the data.

Establishment of an Ovariectomy (OVX)-Induced OP Mouse Model

Twelve female C57BL/6J specific pathogen-free (SPF) mice (11-week-old) were obtained from the Institute of Zoology, Chinese Academy of Sciences (Beijing, China) and bred in individually ventilated cages with an SPF barrier of 22 ± 2 °C and humidity of 40–70%. All animal experiments were performed according to the rules, regulations, and operational specifications of laboratory animal management and met the ethical requirements for laboratory animals.

Twelve mice were randomly divided into two groups: sham (n = 6 mice) and OVX (n = 6 mice). Classical OVX was performed to construct an OP mouse model. Each mouse in the OVX group was anesthetized *via* an intraperitoneal injection of 100 mg/kg ketamine and 10 mg/kg xylazine. Subsequently, ophthalmic scissors were used to cut off 1/3 of the hair in the middle and lower parts of the backs of the mice. After the mice were placed in the prone position, the skin of the surgical area was disinfected with iodophor. Subsequently, a longitudinal incision (approximately 0.5 cm) was made on both sides of the back. Then, the white adipose tissue around the ovary was removed, and the ovary was removed using small forceps. Next, the fallopian tube was ligated, and the incisions were washed with normal saline and sutured layer-by-layer. For mice in the sham group, only the adipose tissues around the ovary were removed, after which the incisions were rinsed and sutured layer-by-layer. After postoperative disinfection of the incisions with iodophor, the mice were returned to their cages and fed a normal diet.

Micro-computed Tomography (CT)

All collected samples were fixed and subjected to micro-CT scanning with the following scanning parameters: 431 μA X-ray tube current and 58 kV voltage. The entire object was scanned with a scanning resolution of 9.00 μm, exposure time of 1000 ms, and a scanning angle of 180°. Thereafter, the 3D reconstruction software, NRecon (V1.7.4.2; Bruker, Karlsruhe, Germany), was used to reconstruct the original figures of the selected area, and a CT analyzer (1.18.8.0; Bruker) was used to analyze the region of interest. The parameters were unified, followed by the measurement of bone mass density (BMD), bone volume/tissue volume (BV/TV), bone surface/bone volume (BS/BV), bone surface/tissue volume (BS/TV), and trabecular number (Tb.N).

Isolation and Culture of BMSCs from Mice

As previously described,[15] the collected bone marrow aspirate from the two groups of mice was carefully removed with a pipette and transferred into a centrifuge tube containing phosphate-buffered saline (PBS) for the preparation of a cell suspensions. Cell suspension was centrifuged at 340 × g for 30 min, followed by the removal of the supernatant. Next, the samples were mixed and suspended in a prepared medium and placed in a culture dish with 10 mL Dulbecco's Modified Eagle Medium (Invitrogen, Carlsbad, CA, USA), 10% fetal bovine serum (FBS; Invitrogen), 10 U/mL penicillin, 10 mg/mL streptomycin (Invitrogen), and 0.5 mg/mL amphotericin B, followed by culture in a constant temperature incubator (37°C, 5% CO_2, and 95% humidity). After three days, adherent cells were defined as BMSCs at passage 0. BMSCs that reached 80–90% confluency in the culture dish were sub-cultured.

Flow Cytometry (FCM)

BMSCs were made into 1.5–2 mL single-cell suspensions (1×10^7 cells/mL) and the expression levels of positive (CD73, CD90, and CD105) and negative (CD34, CD45, and CD19) surface markers for BMSCs were determined *via* FCM, as previously described.[15] Polyethylene-bound CD73, CD90, CD105, CD34, CD45, and CD19 were incubated with cells at 4°C for 30 min in a dark chamber and their expression levels were determined using the FACSCanto type II FCM system. We found that CD73, CD90, and CD105 were positive, whereas CD19, CD34, and CD45 were negative surface markers for BMSCs.

Cell Transfection

ASPN knockdown lentivirus vector [short hairpin (sh)-ASPN: GGTCTGACATCGGTTCCAAAC], HAPLN1 knockdown lentivirus vector (sh-HAPLN1: GCTTCTCCTGGTGCTGATTTC), and their negative control (NC) (sh-NC; 20 μL) were purchased from GenePharma (Shanghai, China) and transfected into BMSCs or bone marrow macrophages (BMMs) for 48 h for subsequent experiments.

Induction of Osteogenic Differentiation

BMSCs were seeded in a 12-well plate and cultured in α-minimum essential medium (α-MEM; Gibco, Grand Island, NY, USA) containing 10% FBS (Gibco), 10 mM sodium β-glycerophosphate (Merck KGaA, Darmstadt, Germany), 250 μM ascorbic acid (Merck KGaA), and 100 nM dexamethasone (Topscience, Shanghai, China). After a seven-day culture, the cells were subjected to alkaline phosphatase (ALP) staining and ALP activity examination. Protein expression levels of ossification marker genes were determined on the 14th day, and alizarin red staining was performed on the 21st day of culture.

ALP Staining and Activity Measurement

After 7 days of osteogenic differentiation induction, BMSCs were washed with PBS and mixed with 1% Triton X-100 for 15 min. Afterwards, cell lysates were centrifuged, and the supernatants were acquired for the analysis of ALP activity. ALP activity was calculated by measurement of the optical density (OD) at 405 nm in triplicate using an ALP detection kit (Abcam, Cambridge, UK) on a microplate reader (Promega, Madison, WI, USA). To calculate the relative activity, the mean value of ALP activity in the control group (OD values at 405 nm) was considered as 1, and the relative ALP activity of other groups was the ratio of OD values in the corresponding group to the mean OD value in the control group.

ALP staining was conducted using an ALP staining kit (Wuhan Carnoss Technology Co., Ltd., Wuhan, China) containing a cleaning solution (Reagent A), fixation solution (Reagent B), and reaction solution (Reagent C), which were added to the samples according to the kit protocols, followed by microscopic observation and photography.

Alizarin Red Staining

After 21 days of induction of osteogenic differentiation, the medium was discarded, followed by twice or thrice washing with PBS. After discarding PBS, 4% paraformaldehyde was added to fix the cells for 15 min at room temperature. The fixation solution was removed, cells were washed with ddH_2O and stained with alizarin red solution (Beyotime, Shanghai, China) for 30 min at room temperature. After the removal of the staining solution and washing with ddH_2O, a microscope (IX50; Olympus, Tokyo, Japan) was used to observe and photograph the cells.

Adipogenic Differentiation Induction and Oil Red O (ORO) Staining

BMSCs were seeded into a 12-well plate. After the cells grew and covered the plates, adipogenic differentiation induction was carried out in an α-MEM/10% FBS containing 0.1 mmol/L rosiglitazone, 10 μg/mL insulin, 0.5 mmol/L IBMX, and 1 μmol/L dexamethasone.[16] The medium was renewed every 2 days. After the induction of adipogenic differentiation, ORO staining was performed. Specifically, the cells were fixed with 10% formalin (15 min), gently washed with ddH_2O, and then washed with 60% isopropanol. Cells were stained with ORO (Beyotime) for 15 min and separately washed with 60% isopropanol and ddH_2O. Finally, water remaining in the medium was removed, and the cells were photographed.

In Vitro Culture and Differentiation of BMMs

Mouse bone marrow aspirates were carefully collected using a pipette and transferred to a centrifuge tubes containing PBS to prepare cell suspensions. Cell suspensions were then transferred into a 50-mL centrifuge tube and centrifuged at 800 × g for 3 min. Following the removal of the supernatant, samples were re-suspended in 10 mL PBS, and the cell suspensions were seeded into a culture dish containing α-MEM. After 24 h, non-adherent cells in the supernatants were obtained *via* 5-min centrifugation at 800 × g, followed by

the discarding of the supernatants. Cells were re-suspended in α-MEM with 10 ng/mL monocyte colony-stimulating factor (M-CSF) and seeded in a culture plate. After the cells adhered to and covered the walls of the wells, the medium was renewed every 2 days, and BMMs were seeded in a 24-well plates at 2×10^6 cells/well and supplemented with α-MEM, M-CSF (final concentration, 25 ng/mL), and receptor activator of nuclear factor-kappa B ligand (final concentration, 0 ng/mL). The medium was refreshed every 2 days. OCs were formed on days 5–7 and subjected to Tartrate-Resistant Acid Phosphatase (TRAP) staining.[17]

Tartrate-Resistant Acid Phosphatase (TRAP) Staining

After euthanasia, the femurs of mice were obtained and placed in 10 mL of precooled ethylene diamine tetraacetic acid decalcifying solution, followed by continuous shaking at 4°C. The decalcifying solution was renewed twice a week, and decalcification lasted for 3 weeks. After decalcification, the femurs were sectioned into paraffin slices. After dehydration, clearing, wax impregnation, and embedding, the samples were cut into 5-μm slices. After cooling, slices were dewaxed, hydrated, and stained with TRAP using a TRAP staining kit, according to the manufacturer's instructions. Under an optical microscope, TRAP-positive cells with at least three nuclei were identified as osteoclasts (OCs). Likewise, after osteoclast differentiation in BMMs, TRAP staining was also conducted as per the instructions of the TRAP staining kit.

Quantitative Reverse Transcription-Polymerase Chain Reaction (qRT-PCR)

Total RNA was isolated using the TRIzol reagent (15,596,026; Invitrogen) and reverse transcribed into cDNA using a reverse transcription kit (RR047A; Takara, Tokyo, Japan). Samples were subjected to qRT-PCR on a real-time fluorescence quantification PCR instrument (ABI7500; Applied Biosystems, Foster City, CA, USA) using the following reaction system: 9 μL SYBR Mix, 0.5 μL positive primers, 5 μL negative primers, 2 μL cDNA, and 8 μL RNase-free H_2O. Reaction conditions were 10 min at 95°C, 40 cycles of 15 s at 95°C, and 1 min at 60°C. Three duplicate wells were used for each sample. Primers were synthesized by Sangon Biotech (Shanghai, China; Table 1). Ct values for each well were recorded. Glyceraldehyde-3-phosphate dehydrogenase (GAPDH) was used as an internal reference, and $2^{-\Delta\Delta Ct}$ method was used to calculate the relative expression levels of the products. ΔΔCt = (mean Ct value of target gene in the experimental group—mean Ct value of housekeeping gene in the experimental group)—(mean Ct value of target gene in the control group—mean Ct value of housekeeping gene in the control group). The experiment was repeated three times.

TABLE 1 Primer sequences

Name of primer	Sequences (5′-3′)
ASPN-F	CTCTGACAAGGCCAGCATGAA
ASPN-R	AGGGTTCACTGGCTCTTTCG
HAPLN1-F	GCATGGAGTGCAGTTAGGCT
HAPLN1-R	GAAAGGCAAAGCGTCACCAG
GAPDH-F	CCCTTAAGAGGGATGCTGCC
GAPDH-R	ACTGTGCCGTTGAATTTGCC

Abbreviations: ASPN, asporin; F, forward; GAPDH, glyceraldehyde-3-phosphate dehydrogenase; HAPLN1, hyaluronan and proteoglycan link protein 1; R, reverse.

Western Blotting

Cells or tissues were washed with pre-cooled PBS and lysed with a protein extraction lysis buffer. A bicinchoninic acid kit (Beyotime) was used to estimate protein concentration. Corresponding volume of protein was evenly mixed with the loading buffer (Beyotime). Then, the proteins were denatured by heating for 3 min in a boiling water bath. After 30-min of electrophoresis at 80 V, the voltage was changed to 120 V for another 1–2 h of electrophoresis when bromophenol blue entered the separation gel. The proteins were transferred to a membrane in an ice bath at 300 mA for 60 min, after which the membrane was rinsed for 1–2 min and then sealed in a blocking buffer for 60 min at room temperature or overnight at 4°C. Under room temperature, the membrane was incubated with primary antibodies against GAPDH (ab9485; 1:2500; Abcam), ASPN (ab31303; 1:1000; Abcam), osteopontin (OPN; ab63856; 1:1000; Abcam), osteocalcin (OCN; ab93876; 1:1000; Abcam), collagen type I alpha 1 chain (COL1A1; ab260043; 1:1000; Abcam), nuclear factor of activated T cells 1 (Nfatc1; ab25916; 1:1000; Abcam), c-Fos (1:1000; ab222699), and HAPLN1 (MA5-32100; 1:1000; Thermo Fisher Scientific, Waltham, MA, USA) for 1 h in a shaking incubator. After three washes (10 min each), the membrane was incubated with secondary antibodies [Immunoglobulin G (IgG), 1:10000; Abcam] for 1 h at room temperature and washed thrice (10 min each). Following dropwise addition of a developer, a chemiluminescence imaging system (Bio-Rad, Hercules, CA, USA) was used for detection. The experiment was repeated three times.

Co-Immunoprecipitation (co-IP) Assay

Precooled Radio-Immunoprecipitation assay (RIPA) cell lysis buffer was added to lyse the cells, followed by 15-min centrifugation at 4°C and 14 000 × *g*. Next, the supernatant was transferred to a new centrifugation tube and one lysate was added to 1 μg of the antibody (ASPN [PAC321Mu02]; Cloud-Clone Corp., Wuhan, China) or IgG antibodies (NC group) and cultured in a shaker incubator overnight at 4°C or slowly shaken for 2 h at room temperature. Next, 100 μL of protein A/G agarose beads (prepared with PBS to a concentration of 50%) were added to capture the antigen–antibody complexes, which were slowly shaken overnight at 4°C or incubated for 1 h at room temperature. After 5 s of transient centrifugation at 14 000 rpm, the supernatant was removed, and agarose bead-antigen–antibody complexes

were obtained. After washing thrice with 800 μL precooled RIPA buffer, 60 μL of 2 × loading buffer was used to suspend the agarose bead-antigen–antibody complexes and evenly mixed. The loading samples underwent 5-min boiling and centrifugation at 14 000 × g to collect the remaining agarose beads. After protein denaturation *via* 5-min boiling, the supernatant was subjected to electrophoresis and western blotting to determine the protein expression levels of HAPLN1.

Glutathione S-Transferase (GST) Pull-Down Assay

Ambition Biotechnology (Beijing, China) constructed GST and HAPLN1-GST in *Escherichia coli* BL21 (American Type Culture Collection, Manassas, VA, USA). Positive clones were selected, and prokaryotic expression was induced using isopropyl-β-d-thiogalactoside. Then, HAPLN1–GST fusion proteins were subjected to affinity chromatography purification using glutathione agarose columns. Purified HAPLN1-GST fusion proteins, GST-labeled proteins, and GST-beads (Biomag Biotechnology, Wuxi, China) were mixed in an Eppendorf (EP) tube and rotated in a chromatography cabinet at 4°C for 1 h for binding. Cells transfected with ASPN were collected and fully lysed, after which 20% volume of liquid was utilized as input (positive control) and the rest of the supernatant was added into the aforementioned EP tube and rotated for 4 h in a chromatography cabinet at 4°C for binding. Subsequently, GST-beads were washed thrice and analyzed *via* western blotting using ASPN antibodies. Additionally, a 2% volume of the mixture was used for western blotting analysis of the expression levels of each component.

Statistical Analysis

GraphPad Prism v8.0 software (GraphPad Prism, CA, USA) was used for all statistical analyses. Data are represented as the mean ± standard deviation. For samples with normal distribution, *t*-test was used for two-group comparisons and one-way analysis of variance was used for multiple-group comparisons. Tukey's test was adopted for post-hoc multiple comparisons. For samples without normal distribution, the Mann–Whitney *U* test was used to analyze the two independent samples, and the Kruskal–Wallis test was used to analyze multiple independent samples. Statistical significance was set at $P < 0.05$.

Results

ASPN and HAPLN1 Expression Levels Were Upregulated in Patients with OP

GSE156508 was downloaded from the GEO database to screen for differentially expressed genes in OBs of patients with OP (Fig. 1A). Differentially expressed genes with $|\log FC| > 1$ and $P < 0.05$ were selected and predicted with STRING and protein interactions were observed between ASPN and HAPLN1 (Fig. 1B). Moreover, PathCard revealed that ASPN and HAPLN1 are both associated with ECM (Fig. 1C). These data indicate the potential effects of ASPN and HAPLN1 on OP.

ASPN and HAPLN1 Were Highly Expressed in Bone Tissues of OVX Mice

Post-menopausal OP mouse model was constructed *via* OVX and micro-CT was used to scan and analyze the femurs of mice. Moreover, microarchitecture of the distal trabecular bone was assessed by the determination of its morphologic parameters, including BMD, BV/TV, BS/BV, BS/TV, and Tb. N. We observed a reticular trabecular bone structure in the distal femurs of sham-operated mice and found that the trabecular bones in distal femurs were significantly sparser in OVX mice than in sham-operated mice (Fig. 2A). Compared with the sham group, the BS/BV value of mice significantly increased. Whereas the values of all other parameters significantly decreased in the OVX group (Fig. 2B). TRAP staining indicated significantly increased OC levels in the femurs of OVX mice than in the sham-operated mice (Fig. 2C). Western blotting revealed that OPN, OCN, and COL1A1 expression levels in bone tissues were significantly decreased in the OVX group than in the sham group (Fig. 2D). These findings confirmed the successful establishment of the OP mouse model. qRT-PCR and western blotting revealed significantly increased expression levels of ASPN and HAPLN1 in OVX mice (Fig. 2E,F). These findings indicate that ASPN and HAPLN1 expression levels are increased in OVX mice.

ASPN Interacted with HAPLN1 in BMSCs of OVX Mice

FCM revealed positive expression of CD73, CD90, and CD105, and negative expression of CD34, CD45, and CD19 in BMSCs (Fig. 3A). BMSCs were subjected to ORO staining after the induction of adipogenic differentiation (Fig. 3B). BMSCs were found to differentiate into adipose cells with stronger adipogenesis abilities in the OVX group than in the sham group. Twenty-one days after osteogenic differentiation induction, alizarin red staining revealed that BMSCs formed mineralized nodules and that the degree of mineralization in the OVX group was lower than that in the sham group (Fig. 3C). To determine whether ASPN and HAPLN1 interacted with each other, Co-IP was first used to detect the binding of ASPN to HAPLN1 in BMSCs of OVX mice, which revealed that ASPN antibodies enriched the HAPLN1 protein (Fig. 3D). GST pull-down assay further verified the direct interaction between ASPN and HAPLN1 (Fig. 3E). These results confirm the interaction between ASPN and HAPLN1 in BMSCs of OVX mice.

ASPN and HAPLN1 Knockdown Promoted the Osteogenic Differentiation of BMSCs and ECM Mineralization of OBs

BMSCs of OVX mice were transfected with sh-ASPN, sh-HAPLN1, or NC. qRT-PCR and western blotting revealed that ASPN and HAPLN1 expression levels were significantly downregulated in the sh-ASPN + sh-NC group than in the

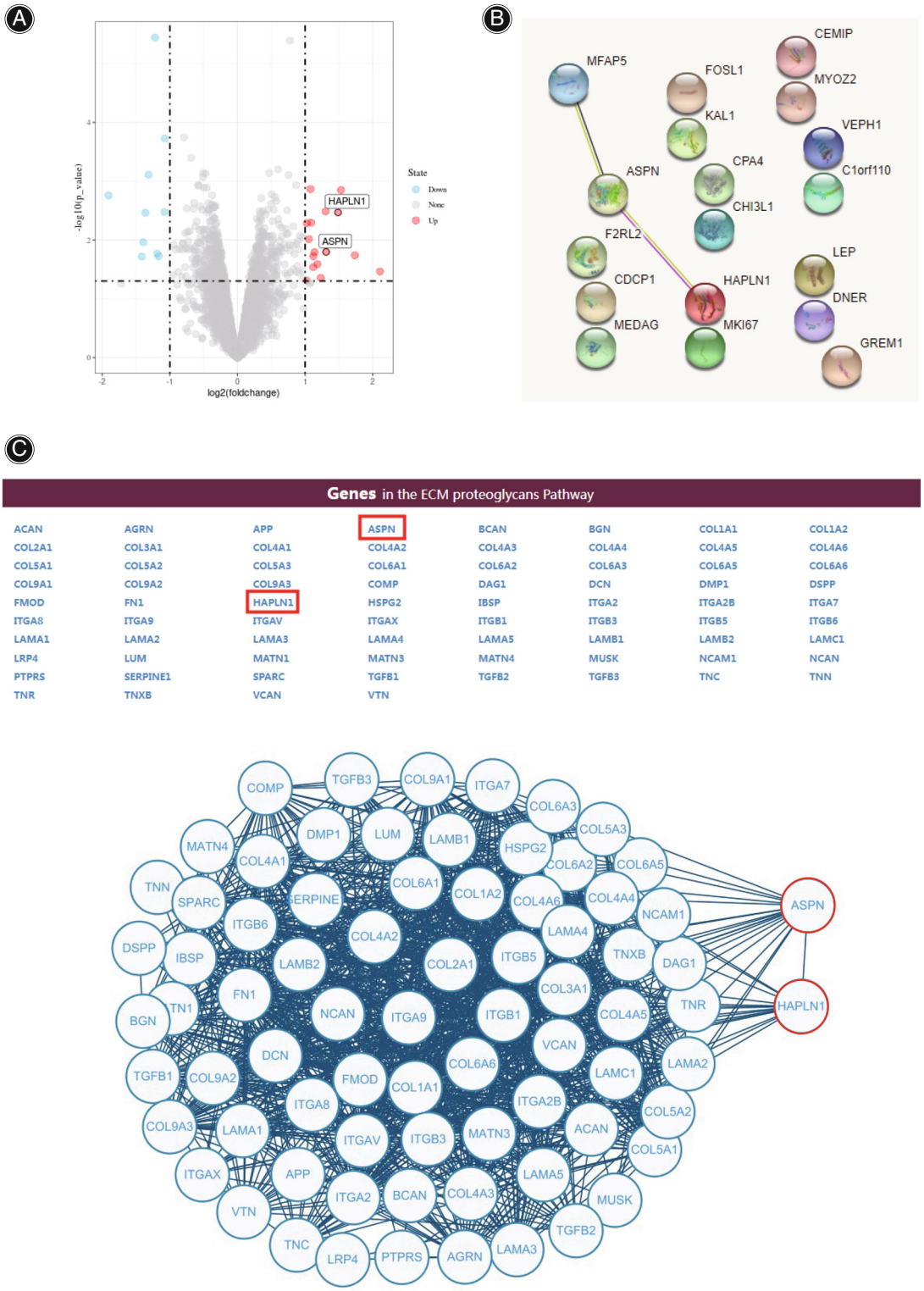

Fig. 1 ASPN and HAPLN1 are highly expressed in patients with OP. (A) The expression of differential genes in GSE156508 dataset; (B) STRING database prediction of the protein interaction between ASPN and HAPLN1; (C) PathCard prediction of genes related to ECM and the corresponding map plotted with cytoscape. ASPN, asporin; HAPLN, hyaluronan and proteoglycan link protein; OP, osteoporosis; GSE, GEO Series; GEO, gene expression omnibus; ECM, extracellular matrix

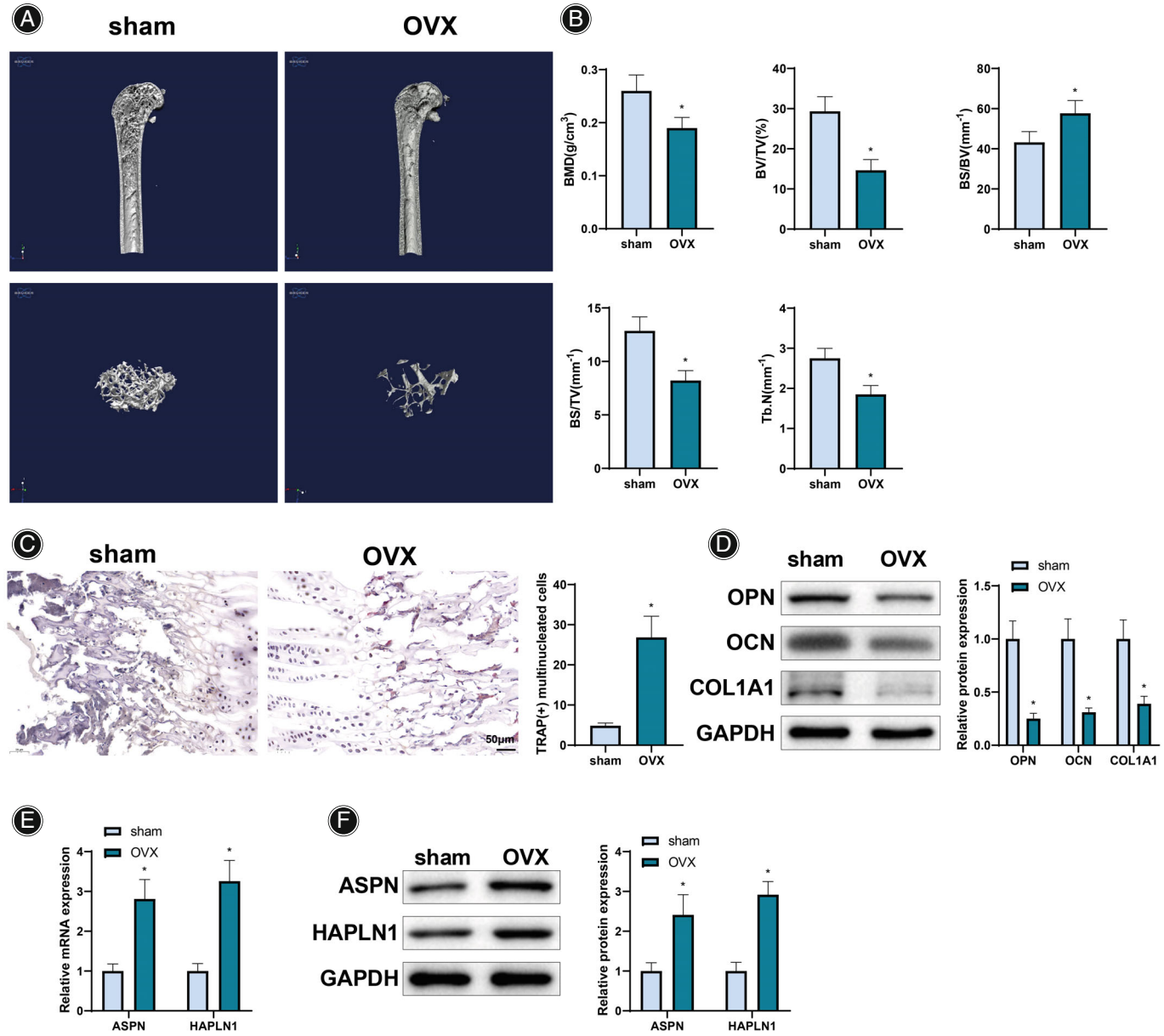

Fig. 2 ASPN and HAPLN1 expression is high in OVX mice. (A) Micro-CT scanning of trabecular bone morphology in the distal femur of mice; (B) Morphologic parameters of trabecular bones in the distal femurs of mice; (C) TRAP staining; (D) Western blot detection of OPN, OCN, and COL1A1 expression in bone tissues of mice; (E-F) qRT-PCR (D) and western blot (E) to detect ASPN and HAPLN1 expression in bone tissues of mice. N = 6 mice/group, * $P < 0.05$ *versus* the sham group. ASPN, asporin; HAPLN, hyaluronan and proteoglycan link protein; OVX, ovariectomy; CT, computed tomography; TRAP, tartrate resistant acid phosphatase; qRT-PCR, quantitative reverse transcription polymerase chain reaction; OPN, osteopontin; OCN, osteocalcin; COL1A1, collagen type I alpha 1 chain

sh-NC group. The sh-HAPLN1 + sh-NC group exhibited a significant decrease in HAPLN1 levels, but the difference in ASPN levels was insignificant compared to that in the sh-NC group. HAPLN1 levels were significantly downregulated in the sh-ASPN + sh-HAPLN1 group than in the sh-ASPN + sh-NC group. HAPLN1 and ASPN levels were significantly decreased in the sh-ASPN + sh-HAPLN1 group than in the sh-HAPLN1 + sh-NC group (Fig. 4A–D). On the 7th day of osteogenic differentiation induction in BMSCs, ALP levels were significantly increased in the sh-ASPN + sh-NC and sh-HAPLN1 + sh-NC groups *vs* the sh-NC group and the sh-ASPN + sh-HAPLN1 group *vs* the sh-ASPN + sh-NC or sh-HAPLN1 + sh-NC group (Fig. 4E,F). On the 14th day of culture, OPN, OCN, and COL1A1 expression levels were

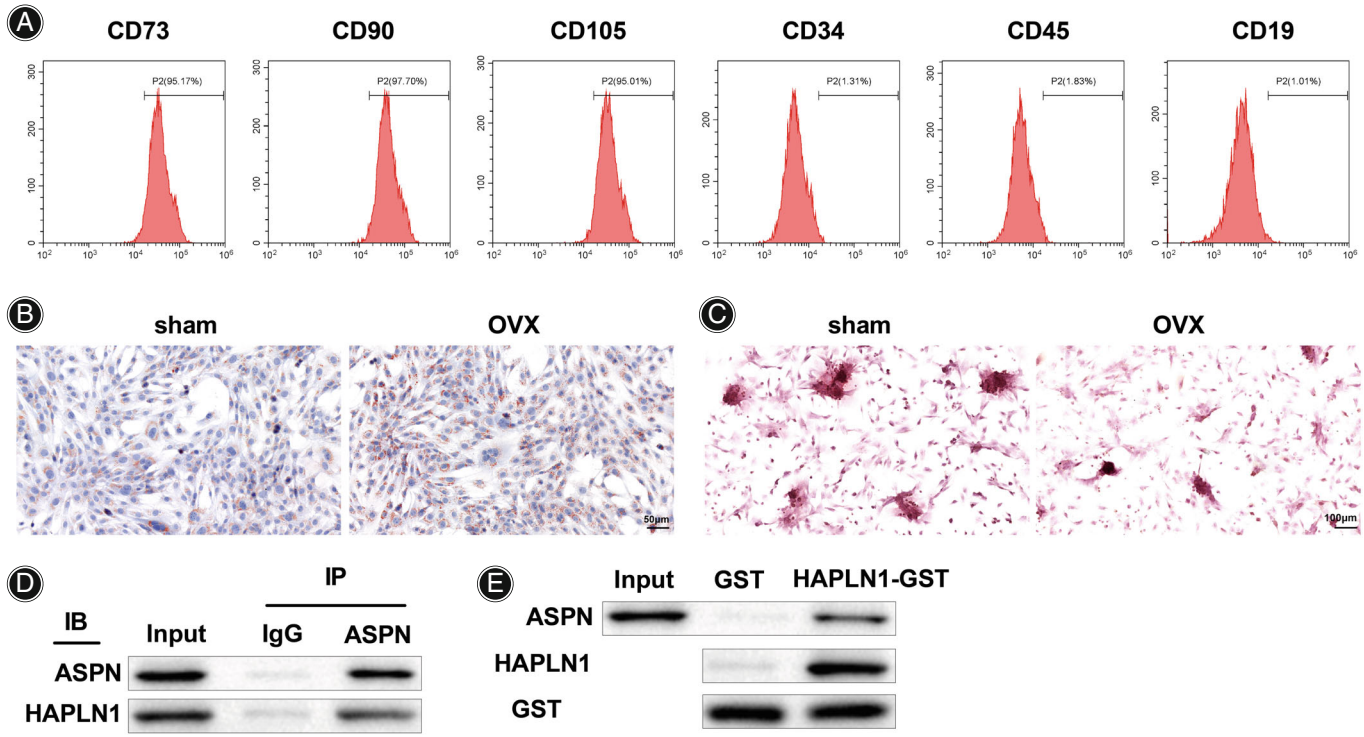

Fig. 3 ASPN interacts with HAPLN1 in BMSCs of OVX mice. (A) FCM detection of CD73, CD90, CD105, CD34, CD45, and CD19 expression in BMSCs; (B) ORO staining after adipogenic differentiation induction of BMSCs; (C) Alizarin red staining on the 21st day of osteogenic differentiation induction of BMSCs; (D-E) Co-IP (D) and GST pull-down (E) assays to monitor binding of ASPN to HAPLN1. ASPN, asporin; HAPLN, hyaluronan and proteoglycan link protein; BMSC, bone marrow stromal cell; OVX, ovariectomy; FCM, flow cytometry; ORO, oil red O; Co-IP, coimmunoprecipitation; GST, glutathione S-transferase

determined. We found that OPN, OCN, and COL1A1 expression levels were significantly increased in the sh-ASPN + sh-NC and sh-HAPLN1 + sh-NC groups than in the sh-NC group. Likewise, the sh-ASPN + sh-HAPLN1 group exhibited significant upregulation of OPN, OCN, and COL1A1 expression levels compared to those in the sh-ASPN + sh-NC and sh-HAPLN1 + sh-NC groups (Fig. 4G). On the 21st day of differentiation, alizarin red staining revealed that the knockdown of ASPN or HAPLN1 increased ECM mineralization, which was further enhanced by the simultaneous knockdown of ASPN and HAPLN1 (Fig. 4H). Therefore, ASPN and HAPLN1 knockdown promote the osteogenic differentiation of BMSCs and ECM mineralization of OBs.

ASPN and HAPLN1 Promoted the Osteoclastogenesis of BMMs

BMMs were isolated from mice in the OVX group and then transfected with sh-ASPN, sh-HAPLN1, and their NC. RT-PCR and western blotting revealed that, compared with the sh-NC group, expression levels of ASPN and HAPLN1 were significantly downregulated in the sh-ASPN + sh-NC group, whereas HAPLN1 levels were decreased and ASPN levels were insignificantly affected in the sh-HAPLN1 + sh-NC group. Moreover, the sh-ASPN + sh-HAPLN1 group exhibited significantly decreased HAPLN1 expression levels compared to those in the sh-ASPN + sh-NC group and significantly decreased ASPN and HAPLN1 expression levels compared to those in the sh-HAPLN1 + sh-NC group (Fig. 5A,B). TRAP staining after osteoclastogenesis induction revealed decreased number of OCs in the sh-ASPN + sh-NC and sh-HAPLN1 + sh-NC groups than in the sh-NC group, and this number was further decreased in the sh-ASPN + sh-HAPLN1 group than in the sh-ASPN + sh-NC or sh-HAPLN1 + sh-NC group (Fig. 5C). Western blotting revealed decreased Nfatc1 and c-Fos expression levels in the sh-ASPN + sh-NC or sh-HAPLN1 + sh-NC group *vs* the sh-NC group and the sh-ASPN + sh-HAPLN1 group *vs* the sh-ASPN + sh-NC or sh-HAPLN1 + sh-NC group (Fig. 5D).

Discussion

ECM mineralization and osteogenic differentiation participate in bone formation and manipulate the progression of the common systemic skeletal disorder OP which attracts attention for its prevention and therapy.[18–20] Several studies have focused on the molecular mechanisms underlying the osteogenic differentiation of BMSCs and ECM mineralization of OBs to identify the OP-related mechanisms.[21–23] In this

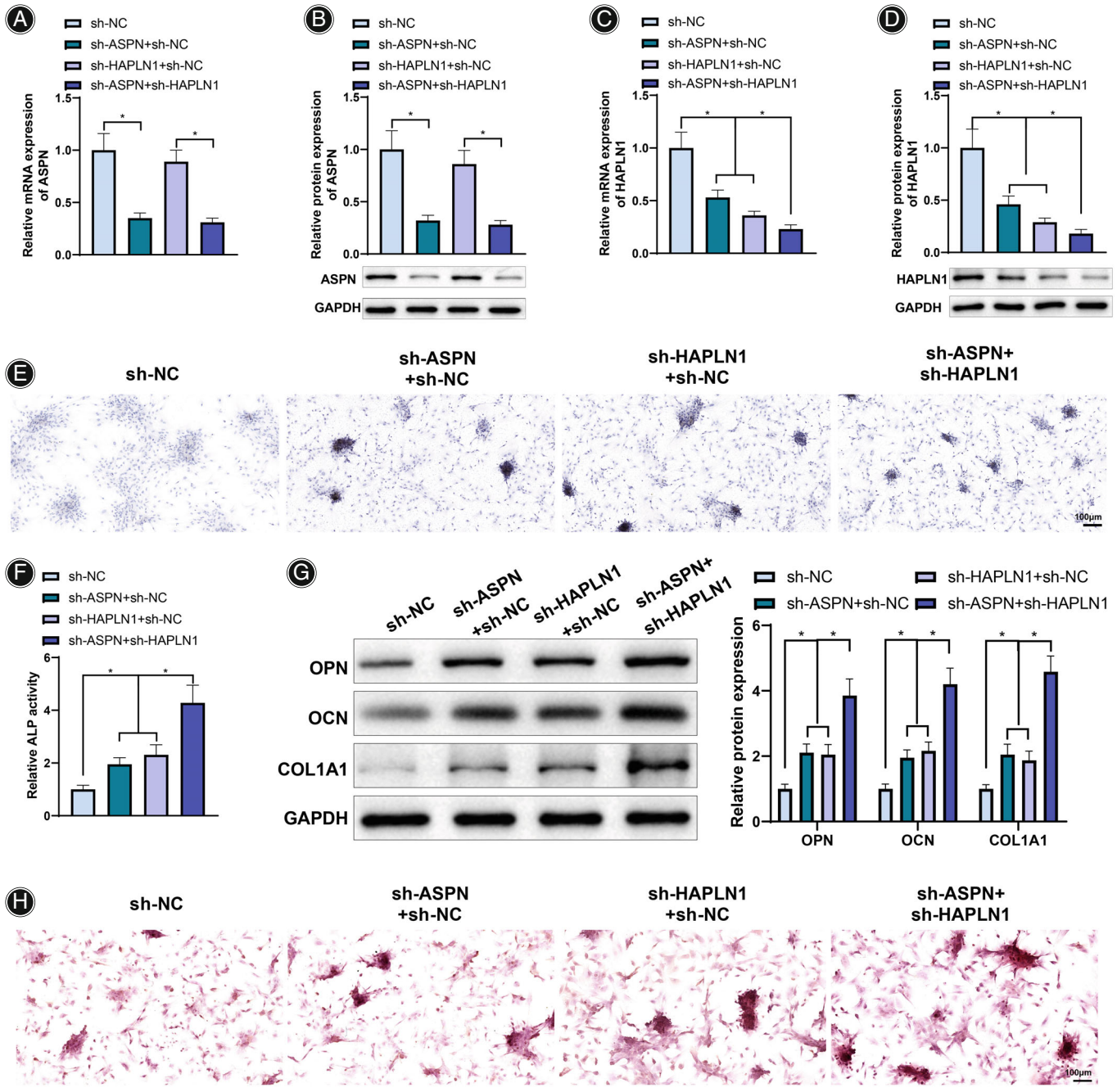

Fig. 4 ASPN and HAPLN1 knockdown facilitates osteogenic differentiation of BMSCs and ECM mineralization of OBs. BMSCs were transfected with sh-ASPN, sh-HAPLN1, and their NC. (A-D) qRT-PCR and western blot detection of ASPN and HAPLN1 expression; (E-F) ALP staining and ALP activity examination on the 7th day of osteogenic differentiation induction of BMSCs; (G) Western blot assessment of OPN, OCN, and COL1A1 expression on the 14th day of osteogenic differentiation induction of BMSCs; (H) Alizarin red staining on the 21st day of osteogenic differentiation induction of BMSCs. * $P < 0.05$ *versus* the sh-NC, sh-ASPN + sh-NC, or sh-HAPLN1 + sh-NC group. The experiments were repeated 3 times. ASPN, asporin; HAPLN, hyaluronan and proteoglycan link protein; BMSC, bone marrow stromal cell; ECM, extracellular matrix; Sh, short hairpin; NC, negative control; qRT-PCR, quantitative reverse transcription polymerase chain reaction; ALP, alkaline phosphatase; OPN, osteopontin; OCN, osteocalcin; COL1A1, collagen type I alpha 1 chain; Nfatc1, nuclear factor of activated T cells 1; OB, osteoblast

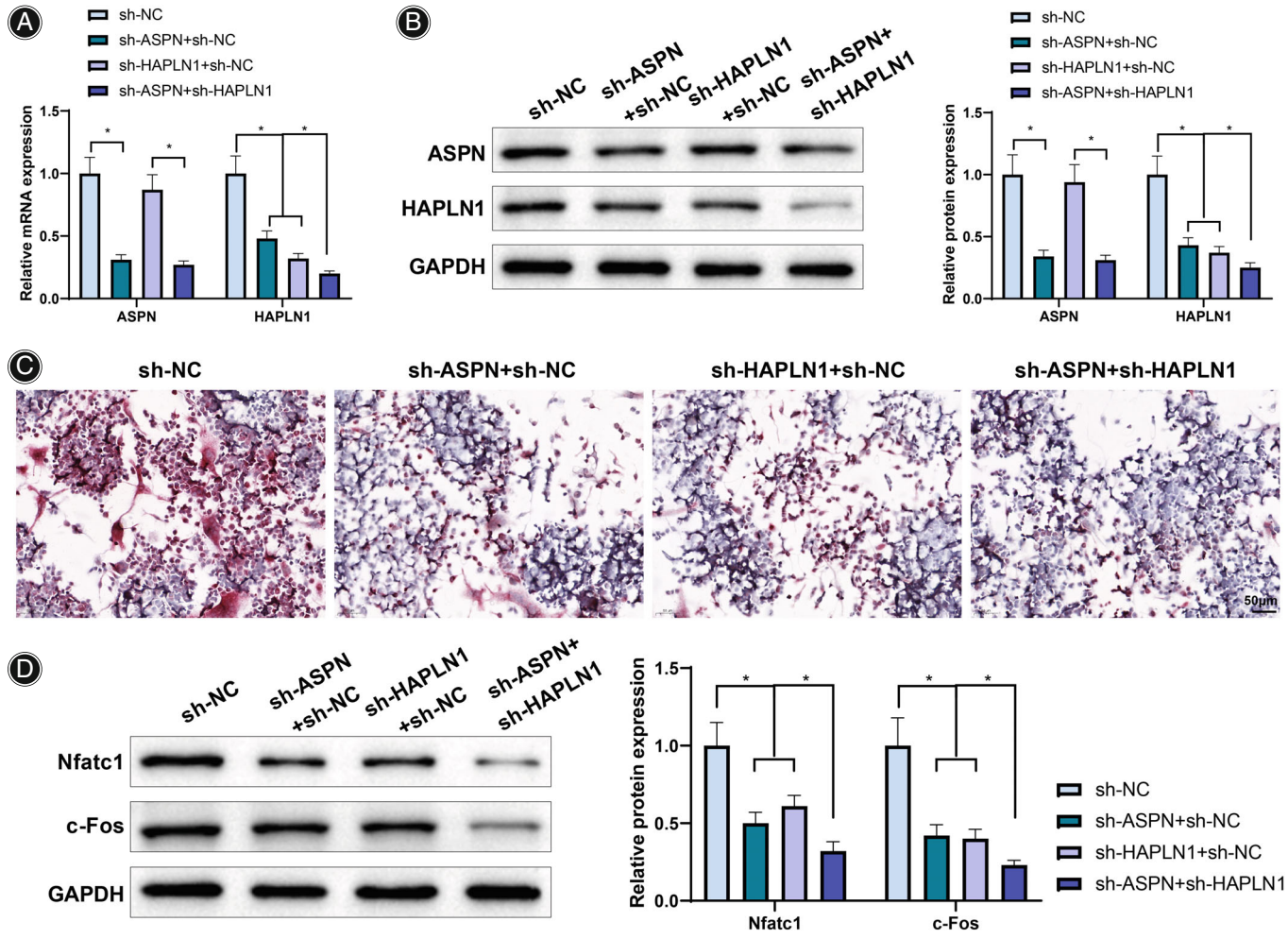

Fig. 5 ASPN and HAPLN1 facilitate osteoclastogenesis of BMMs. Sh-ASPN, sh-HAPLN1, and their NC were transfected into BMMs from mice in the OVX group. (A-B) qRT-PCR and western blot to evaluate the expression of ASPN and HAPLN1 in BMMs; (C) TRAP staining results; (D) Western blot to determine the expression of Nfatc1 and c-Fos in BMMs. * $P < 0.05$. The experiment was repeated 3 times. ASPN, asporin; HAPLN, hyaluronan and proteoglycan link protein; BMMs, bone marrow macrophages; Sh, short hairpin; NC, negative control; OVX, ovariectomy; qRT-PCR, quantitative reverse transcription polymerase chain reaction; TRAP, tartrate resistant acid phosphatase; Nfatc1, nuclear factor of activated T cells 1

study, we determined the effects of ASPN and HAPLN1 on the osteogenic differentiation of BMSCs and ECM mineralization of OBs to uncover the underlying molecular mechanisms.

Main Findings of this Study

We concluded in our research findings that: (i) An OP mouse model was successfully established, and ASPN and HAPLN1 are highly expressed in OP patients and bone tissues of OP model mice; (ii) ASPN/HAPLN1 inhibits osteogenic differentiation and ECM mineralization in BMSCs, and facilitates osteoclastogenesis of BMMs; and (iii) ASPN synergizes with HAPLN1 to suppress the osteogenic differentiation of BMSCs and ECM mineralization of OBs.

High Expression of ASPN and HAPLN1 in OP

OVX is widely used to establish OP models.[24–26] Here, we used this method to successfully induce an OP mouse model with increased BS/BV values and number of OCs and decreased BMD, BV/TV, and BS/TV values and OPN, OCN, and COL1A1 expression levels. BMSCs were extracted from the OVX mice for experiments. ASPN and HAPLN1 have been reported to inhibit bone formation and involved in skeletal diseases.[27–30] ASPN levels were upregulated in degenerate discs and temporomandibular joint internal derangement and glucocorticoid-induced OP.[5,8,31] Likewise, HAPLN1 expression levels are upregulated in axial spondyloarthritis and rheumatoid arthritis.[32,33] These reports indicate the pathogenic potential of both ASPN and HAPLN1 in OP. Therefore, we detected the expression of both genes to prove it. Accordingly, in our

study, we identified that ASPN and HAPLN1 expression levels were increased in OBs of patients with OP (through GSE156508 dataset) and in OVX-induced OP mice.

Roles of ASPN and HAPLN1 in OP

PathCard prediction revealed the association of ASPN and HAPLN1 with ECM. In addition, a previous study recorded that ASPN was involved in the modulation of cardiac ECM in cardiac remodeling.[34] HAPLN1 was also reported to be associated with the ECM function in the neuron system.[35] Considering the close linkage of ECM mineralization to bone loss and the aforementioned results, we determined the specific effects of ASPN and HAPLN1 on the osteogenic differentiation of BMSCs and ECM mineralization of OBs. OPN is a secreted phosphoprotein involved in the progression of bone diseases.[36] OCN is an OB-derived factor that regulates bone mineralization.[37] COL1A1 is a protein that influences bone growth.[38] Hence, we utilized these indexes for related detections and found that ASPN knockdown increased COL1A1, OCN, and OPN expression levels, ALP activity, and ECM mineralization in BMSCs of OVX mice. Kajikawa *et al.* also reported that ASPN treatment inhibited ALP intensity and activity and decreased the expression levels of osteogenesis-related COL1A1, thereby inhibiting the cytodifferentiation and mineralization of periodontal ligament cells.[39] Another study reported that ASPN overexpression decreased OCN expression in rat periodontal bone defects.[40] The just-mentioned documentations further increased the credibility of our results. Meanwhile, a decrease in HAPLN1 expression was accompanied by an increase in COL1A1 expression in damaged cartilage,[41] which indirectly supports our finding in this study that COL1A1 expression was upregulated after HAPLN1 knockdown in BMSCs of OVX mice. In addition, our data revealed that HAPLN1 knockdown increased the ALP activity, OPN and OCN expression levels, and ECM mineralization in BMSCs of OVX mice. We also determined the levels of osteoclastic differentiation-related proteins, Nfatc1 and c-Fos in BMMs[17,42] to verify our findings. We found that ASPN or HAPLN1 knockdown decreased Nfatc1 and c-Fos expression levels in BMMs, indicating their inhibitory effects on osteoclastic differentiation, which has barely been mentioned in existing literature and warrants following evaluation in future research.

Synergistic Effects of ASPN and HAPLN1 in OP

Except for the fact that little is known about the interactions between ASPN and HAPLN1, we discovered that STRING predicted an interaction between ASPN and HAPLN1, which was validated by our Co-IP and GST pull-down assays. As a result, the co-treatment of ASPN and HAPLN1 was performed in our research and it was discerned that compared with the knockdown of ASPN or HAPLN1 alone, simultaneous knockdown of ASPN and HAPLN1 significantly increased the osteogenic differentiation of BMSCs and ECM mineralization of OBs and inhibited osteoclastic differentiation, specifically, the ALP activity, OPN and OCN expression levels, and ECM mineralization in BMSCs were all increased while number of OCs and the expression of Nfatc1 and c-Fos were decreased, suggesting their synergistic roles in OP progression. The coordination of ASPN and HAPLN1 in OP and other disease and their specific interaction mechanisms have barely been probed before. Hence, more research was in need to be promoted to fill in this gap.

Limitations and Strengths of this Study

Our research verified and enriched the findings of molecular regulatory functions on the osteogenic differentiation of BMSCs, ECM mineralization of OBs, and osteoclastogenesis of BMMs, which unveiled the potential candidate targets for the treatment of OP. However, part of our findings lack the evidence support from existing literature and our research data are limited. The downstream pathways were also currently not surveyed. Further explorations in related aspect of mechanisms are needed.

Conclusion

In summary, our findings revealed that ASPN and HAPLN1 knockdown synergistically promotes the osteogenic differentiation of BMSCs and ECM mineralization of OBs and inhibits osteoclastogenesis of BMMs. These findings suggest ASPN and HAPLN1 as candidate targets for OP treatment. Nevertheless, considering the limits of our research data and lack of previous related evidence, more investigations are needed to be carried out to enrich the knowledge of related mechanisms. Additionally, our data revealed that ASPN knockdown decreased HAPLN1 expression but HAPLN1 knockdown had no effect on ASPN expression. Therefore, the specific regulatory mechanisms between ASPN and HAPLN1 in BMSCs need to be investigated further in future studies.

Author Contributions

ZGH and WFQ conceived the ideas. ZGU, WFQ and YXM designed the experiments. ZGH, YXM and CZF performed the experiments. ZGH and WFQ analyzed the data. ZGH and WFQ provided critical materials. ZGH, YXM and ZX wrote the manuscript. WFQ supervised the study. All the authors have read and approved the final version for publication.

Conflict of Interest Statement

The authors report no relationships that could be construed as a conflict of interest.

Availability of Data and Materials

The datasets used or analyzed during the current study are available from the corresponding author on reasonable request.

Ethical Statement

The study protocol was ratified by the Medical Ethics Committee of First People's Hospital of Fuzhou.

References

1. Wang J, Liu S, Li J, Zhao S, Yi Z. Roles for miRNAs in osteogenic differentiation of bone marrow mesenchymal stem cells. Stem Cell Res Ther. 2019;10(1):197.
2. Jing H, Su X, Gao B, Shuai Y, Chen J, Deng Z, et al. Epigenetic inhibition of Wnt pathway suppresses osteogenic differentiation of BMSCs during osteoporosis. Cell Death Dis. 2018;9(2):176.
3. Liu H, Yi X, Tu S, Cheng C, Luo J. Kaempferol promotes BMSC osteogenic differentiation and improves osteoporosis by downregulating miR-10a-3p and upregulating CXCL12. Mol Cell Endocrinol. 2021;520:111074.
4. Alcorta-Sevillano N, Macias I, Infante A, Rodriguez CI. Deciphering the relevance of bone ECM signaling. Cell. 2020;9(12):2630.
5. Ege B, Erdogmus Z, Bozgeyik E, Koparal M, Kurt MY, Gulsun B. Asporin levels in patients with temporomandibular joint disorders. J Oral Rehabil. 2021;48(10): 1109–17.
6. Sakashita H, Yamada S, Kinoshita M, Kajikawa T, Iwayama T, Murakami S. Mice lacking PLAP-1/asporin counteracts high fat diet-induced metabolic disorder and alveolar bone loss by controlling adipose tissue expansion. Sci Rep. 2021; 11(1):4970.
7. Sun J, Zhang T, Zhang P, Lv L, Wang Y, Zhang J, et al. Overexpression of the PLAP-1 gene inhibits the differentiation of BMSCs into osteoblast-like cells. J Mol Histol. 2014;45(5):599–608.
8. Li L, Yang M, Jin A. COL3A1, COL6A3, and SERPINH1 are related to glucocorticoid-induced osteoporosis occurrence according to integrated bioinformatics analysis. Med Sci Monit. 2020;26:e925474.
9. Mayer JE, Iatridis JC, Chan D, Qureshi SA, Gottesman O, Hecht AC. Genetic polymorphisms associated with intervertebral disc degeneration. Spine J. 2013; 13(3):299–317.
10. Evanko SP, Gooden MD, Kang I, Chan CK, Vernon RB, Wight TN. A role for HAPLN1 during phenotypic modulation of human lung fibroblasts in vitro. J Histochem Cytochem. 2020;68(11):797–811.
11. Urano T, Narusawa K, Shiraki M, et al. Single-nucleotide polymorphism in the hyaluronan and proteoglycan link protein 1 (HAPLN1) gene is associated with spinal osteophyte formation and disc degeneration in Japanese women. Eur Spine J. 2011;20(4):572–7.
12. Hunyadi A, Gaal B, Matesz C, et al. Distribution and classification of the extracellular matrix in the olfactory bulb. Brain Struct Funct. 2020;225(1):321–44.
13. Chen Y, Wang B, Chen Y, Wu Q, Lai WF, Wei L, et al. HAPLN1 affects cell viability and promotes the pro-inflammatory phenotype of fibroblast-like synoviocytes. Front Immunol. 2022;13:888612.
14. Belinky F, Nativ N, Stelzer G, et al. PathCards: multi-source consolidation of human biological pathways. Database. 2015;2015:bav006.
15. Brennan MA, Renaud A, Guilloton F, Mebarki M, Trichet V, Sensebé L, et al. Inferior In vivo Osteogenesis and superior angiogenesis of human adipose-derived stem cells compared with bone marrow-derived stem cells cultured in Xeno-free conditions. Stem Cells Transl Med. 2017;6(12):2160–72.
16. Suo J, Zou S, Wang J, Han Y, Zhang L, Lv C, et al. The RNA-binding protein Musashi2 governs osteoblast-adipocyte lineage commitment by suppressing PPARgamma signaling. Bone Res. 2022;10(1):31.
17. Yang Y, Chung MR, Zhou S, Gong X, Xu H, Hong Y, et al. STAT3 controls osteoclast differentiation and bone homeostasis by regulating NFATc1 transcription. J Biol Chem. 2019;294(42):15395–407.
18. Ensrud KE, Crandall CJ. Osteoporosis. Ann Intern Med. 2017;167(3): ITC17–32.
19. Bukhari SNA, Hussain F, Thu HE, Hussain Z. Synergistic effects of combined therapy of curcumin and Fructus Ligustri Lucidi for treatment of osteoporosis: cellular and molecular evidence of enhanced bone formation. J Integr Med. 2019; 17(1):38–45.
20. Guo HL, Wang X, Yang GY, Wu YY, Chen YC, Zhan HS, et al. LINC00472 promotes osteogenic differentiation and alleviates osteoporosis by sponging miR-300 to upregulate the expression of FGFR2. Eur Rev Med Pharmacol Sci. 2020; 24(9):4652–64.
21. Li L, Wang P, Hu K, Wang X, Cai W, Ai C, et al. PFMG1 promotes osteoblast differentiation and prevents osteoporotic bone loss. FASEB J. 2018;32(2):838–49.
22. Liu F, Yuan Y, Bai L, Yuan L, Li L, Liu J, et al. LRRc17 controls BMSC senescence via mitophagy and inhibits the therapeutic effect of BMSCs on ovariectomy-induced bone loss. Redox Biol. 2021;43:101963.
23. Zhang Z, Jiang W, Hu M, Gao R, Zhou X. MiR-486-3p promotes osteogenic differentiation of BMSC by targeting CTNNBIP1 and activating the Wnt/beta-catenin pathway. Biochem Biophys Res Commun. 2021;566: 59–66.
24. Li B, Liu M, Wang Y, Gong S, Yao W, Li W, et al. Puerarin improves the bone micro-environment to inhibit OVX-induced osteoporosis via modulating SCFAs released by the gut microbiota and repairing intestinal mucosal integrity. Biomed Pharmacother. 2020;132:110923.
25. Li J, Li X, Liu D, Hamamura K, Wan Q, Na S, et al. eIF2alpha signaling regulates autophagy of osteoblasts and the development of osteoclasts in OVX mice. Cell Death Dis. 2019;10(12):921.
26. Zhang F, Xie J, Wang G, Zhang G, Yang H. Anti-osteoporosis activity of Sanguinarine in preosteoblast MC3T3-E1 cells and an ovariectomized rat model. J Cell Physiol. 2018;233(6):4626–33.
27. Li J, Wang L, Yu D, Hao J, Zhang L, Adeola AC, et al. Single-cell RNA sequencing reveals thoracolumbar vertebra heterogeneity and rib-genesis in pigs. Genomics Proteomics Bioinformatics. 2021;19(3):423–36.
28. Ueda M, Goto T, Kuroishi KN, Gunjigake KK, Ikeda E, Kataoka S, et al. Asporin in compressed periodontal ligament cells inhibits bone formation. Arch Oral Biol. 2016;62:86–92.
29. Shi D, Dai J, Zhu P, Qin J, Zhu L, Zhu H, et al. Association of the D repeat polymorphism in the ASPN gene with developmental dysplasia of the hip: a case-control study in Han Chinese. Arthritis Res Ther. 2011;13(1):R27.
30. Xu L, Li Z, Liu SY, Xu SY, Ni GX. Asporin and osteoarthritis. Osteoarthr Cartil. 2015;23(6):933–9.
31. Tian W, Zheng S, Jiang XZ, Wu CA, Wang N, Zhao DH. Asporin, a candidate protein for treatment of disc degenerative disease. Chin Med J. 2013;126(2): 369–72.
32. Galligan CL, Baig E, Bykerk V, Keystone EC, Fish EN. Distinctive gene expression signatures in rheumatoid arthritis synovial tissue fibroblast cells: correlates with disease activity. Genes Immun. 2007;8(6):480–91.
33. Layh-Schmitt G, Lu S, Navid F, Brooks SR, Lazowick E, Davis KM, et al. Generation and differentiation of induced pluripotent stem cells reveal ankylosing spondylitis risk gene expression in bone progenitors. Clin Rheumatol. 2017; 36(1):143–54.
34. Huang C, Sharma A, Thakur R, Rai D, Katiki M, Germano JF, et al. Asporin, an extracellular matrix protein, is a beneficial regulator of cardiac remodeling. Matrix Biol. 2022;110:40–59.
35. Szarvas D, Gaal B, Matesz C, Racz E. Distribution of the extracellular matrix in the Pararubral area of the rat. Neuroscience. 2018;394:177–88.
36. Si J, Wang C, Zhang D, Wang B, Zhou Y. Osteopontin in bone metabolism and bone diseases. Med Sci Monit. 2020;26:e919159.
37. Wang JS, Mazur CM, Wein MN. Sclerostin and osteocalcin: candidate bone-produced hormones. Front Endocrinol. 2021;12:584147.
38. Rauch D, Robinson ME, Seiltgens C, Sutton VR, Lee B, Glorieux F, et al. Assessment of longitudinal bone growth in osteogenesis imperfecta using metacarpophalangeal pattern profiles. Bone. 2020;140:115547.
39. Kajikawa T, Yamada S, Tauchi T, Awata T, Yamaba S, Fujihara C, et al. Inhibitory effects of PLAP-1/asporin on periodontal ligament cells. J Dent Res. 2014;93(4):400–5.
40. Yu X, Liu S, Wang W, Li S. Periodontal ligamentassociated protein1 delays rat periodontal bone defect repair by regulating osteogenic differentiation of bone marrow stromal cells and osteoclast activation. Int J Mol Med. 2018;41(2): 1110–8.
41. Dunn SL, Soul J, Anand S, Schwartz JM, Boot-Handford RP, Hardingham TE. Gene expression changes in damaged osteoarthritic cartilage identify a signature of non-chondrogenic and mechanical responses. Osteoarthr Cartil. 2016;24(8): 1431–40.
42. Iwatsuki M, Matsuoka M. Fluoride-induced c-Fos expression in MC3T3-E1 osteoblastic cells. Toxicol Mech Methods. 2016;26(2):132–8.